Systematic Coarse Graining of Environments for the Nonperturbative Simulation of Open Quantum Systems

Nicola Lorenzoni,[1] Namgee Cho,[1] James Lim,[1] Dario Tamascelli,[1,2] Susana F. Huelga,[1,*] and Martin B. Plenio[1,†]

[1]*Institut für Theoretische Physik und IQST, Albert-Einstein-Allee 11, Universität Ulm, D-89081 Ulm, Germany*
[2]*Dipartimento di Fisica "Aldo Pontremoli," Università degli Studi di Milano, Via Celoria 16, 20133 Milano, Italy*

(Received 23 October 2023; revised 22 January 2024; accepted 13 February 2024; published 8 March 2024)

Conducting precise electronic-vibrational dynamics simulations of molecular systems poses significant challenges when dealing with realistic environments composed of numerous vibrational modes. Here, we introduce a technique for the construction of effective phonon spectral densities that capture accurately open-system dynamics over a finite time interval of interest. When combined with existing nonperturbative simulation tools, our approach can reduce significantly the computational costs associated with many-body open-system dynamics.

DOI: 10.1103/PhysRevLett.132.100403

Introduction.—The interaction between electronic and vibrational degrees of freedom governs various dynamical processes in molecular complexes, such as energy and charge transfer [1–9] and chirality-induced spin selectivity [10–13]. This electron-vibrational (vibronic) interaction is typically the result of a quasicontinuous low-frequency vibrational spectrum and several tens of underdamped high-frequency vibrational modes, whose phonon energies are comparable to or larger than the thermal energy at room temperature. Electronic states interact not only with near-resonant vibrational modes [4,14–21], but also with multiple modes over a broad frequency range with vibronic coupling strengths beyond the weak coupling regime. This is the case even for biological photosynthetic pigment-protein complexes (PPCs) [22], where the vibronic coupling is generally weaker than that achievable in engineered molecular systems, such as synthetic dyes and aggregates [23–25].

Vibrational environments characterized by a high degree of structure and extending well beyond the weak coupling regime have made it imperative to employ nonperturbative methods for simulating electronic dynamics and optical responses. Nowadays, a variety of nonperturbative tools designed to address different system types are in widespread use. The time-evolving density operator with orthogonal polynomials algorithm (TEDOPA) [4,26,27] and thermo-field-based chain mapping approaches [28,29] allow us to fully consider highly structured vibrational environments, but they have been applied primarily to small electronic systems such as dimers. The multilayer extension of the multiconfiguration time-dependent Hartree (ML-MCTDH) method [30,31] tackles systems consisting of dozens of electronic states and discrete vibrational modes, typically at zero temperature as computationally expensive statistical sampling is required to account for finite temperature effects. Continuous phonon spectral densities of the spin-boson model at zero temperature have been described by a few hundred discrete modes in the weak coupling regime, but several thousand modes in the strong coupling regime to obtain numerically exact results [32]. For multisite PPCs at zero temperature, the low-energy parts of continuous phonon spectral densities of PPCs have been considered approximately by using several tens of discrete modes per site in ML-MCTDH simulations [33–36], but convergence to the exact results [37] and its extension to full phonon environments remain to be assessed. The time-evolving matrix product operators method [38] and transfer-tensor-TEDOPA [39] yield efficiency improvements when applied to vibrational environments with correlation times shorter than or comparable to the timescale of system dynamics. The hierarchical equation of motion (HEOM) [40] approach has been mainly employed to consider a broad vibronic coupling spectrum consisting of a few peaks, as its computational costs rapidly increase with the number of exponentials in the bath correlation function (BCF). The highly structured vibrational environments of molecular systems have been severely coarse grained in HEOM simulations [41–45] based on two criteria [45]: the conservation of the total vibronic coupling strength, quantified by reorganization energy, and the agreement of monomer absorption spectra computed based on actual and coarse-grained phonon spectral densities, which can be readily computed in a nonperturbative manner. However, the validity of the coarse graining scheme has never been rigorously tested for multi-chromophoric systems using nonperturbative methods.

In this Letter, we leverage the observation that the complexity of the BCF, the key determinant of open-system dynamics, increases with time in the presence of

highly structured spectral densities. We develop a systematic and reliable method for constructing effective environments that describe system dynamics accurately within a chosen finite time interval of interest. When combined with the dissipation-assisted matrix product factorization (DAMPF) [46], a nonperturbative method for simulating open-system dynamics, our approach is capable of capturing the influence of environmental fluctuations on electronic system dynamics, while considerably reducing the computational costs. We demonstrate the efficiency of the method by presenting the absorption spectra of the Fenna-Matthews-Olson (FMO) photosynthetic complex at finite temperature, computed for the first time in an accurate and nonperturbative manner based on experimentally estimated phonon spectral density [47]. Furthermore, we show that conventional coarse graining schemes can fail to reproduce the absorption spectra based on actual vibrational environments, even qualitatively. This underscores the importance of systematically constructing effective environments in open-system simulations. Importantly, our method extends beyond the simulation of absorption, enabling one to reduce the computational costs of nonperturbation simulations of general open-system dynamics.

Model.—Considering a multichromophoric system consisting of N pigments, we express the electronic Hamiltonian within the single excitation subspace as $H_e = \sum_{i=1}^{N} \epsilon_i |\epsilon_i\rangle\langle\epsilon_i| + \sum_{i\neq j}^{N} V_{ij} |\epsilon_i\rangle\langle\epsilon_j|$, where $|\epsilon_i\rangle$ denotes a local electronic excitation of pigment i with site energy ϵ_i and V_{ij} an intrapigment electronic coupling. Here we assume that higher-energy excited states do not contribute to the low-energy part of linear optical spectra, which is a reliable description of PPCs consisting of bacteriochlorophylls such as the FMO complex [3]. Considering an ensemble of PPCs, the site energies ϵ_i of pigments can vary due to nonidentical local environments, resulting in static disorder. This can be addressed by sampling the site energies ϵ_i from independent Gaussian distributions with mean values $\langle\epsilon_i\rangle$ and a standard deviation of σ, here taken as $\sigma = 80\ \mathrm{cm}^{-1}$, a typical value for PPCs [3,22].

The vibronic interaction is modeled by $H_{e-v} = \sum_{i=1}^{N} |\epsilon_i\rangle\langle\epsilon_i| \sum_k \omega_k \sqrt{s_k}(b_{i,k} + b_{i,k}^{\dagger})$, where $b_{i,k}$ and $b_{i,k}^{\dagger}$ denote the annihilation and creation operators, respectively, of a vibrational mode with frequency ω_k, locally coupled to pigment i with a coupling strength quantified by the Huang-Rhys factor s_k. H_{e-v} is fully characterized by a phonon spectral density $J(\omega) = \sum_k \omega_k^2 s_k \delta(\omega - \omega_k)$, and the total vibronic coupling strength is quantified by the reorganization energy $\int_0^{\infty} d\omega J(\omega)/\omega$. In this Letter, we consider the experimentally estimated phonon spectral density of the FMO complex [47] shown in blue in Fig. 1(a), consisting of a quasicontinuous protein spectrum, modeled via the Adolphs-Renger (AR) spectral density $J_{\mathrm{AR}}(\omega)$, and 62 intrapigment vibrational modes, each modeled by a narrow Lorentzian spectral density (see Supplemental Material [48]). Given the vibrational Hamiltonian $H_v = \sum_{i=1}^{N} \sum_k \omega_k b_{i,k}^{\dagger} b_{i,k}$, the total Hamiltonian of the PPC is given by $H = H_e + H_v + H_{e-v}$.

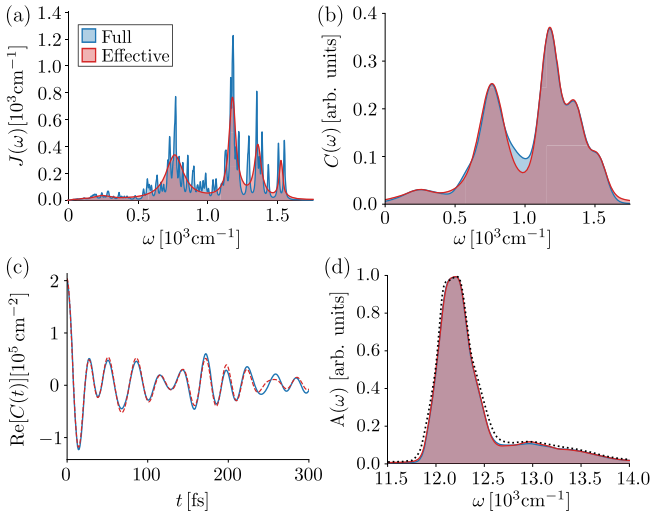

FIG. 1. (a) Experimentally estimated phonon spectral density of the FMO complex [47] (blue) and effective spectral density consisting of six Lorentzian peaks (red). (b) FT spectrum of the Gaussian-filtered BCF of the full FMO spectral density at 77 K (blue) and that of the effective spectral density (red). (c) BCFs of the full FMO (blue) and effective (red) spectral densities without the Gaussian filter. (d) Absorption spectra of a seven-site FMO model at 77 K, computed by DAMPF based on the full FMO (blue) and effective (red) spectral densities where mean site energies and Gaussian broadening were considered (see the main text). The FMO absorption spectra computed based on randomly generated site energies with the effective spectral density are shown as a black dashed line.

BCF-based coarse graining.—Absorption spectra are determined by the time evolution of optical coherences between electronic ground and excited states that are created by external light. The broadening of absorption line shapes is induced by a finite lifetime τ of the optical coherences, determined by vibronic couplings H_{e-v} and static disorder, which is approximately $\tau \approx 300$ fs for the FMO complex and dimeric systems at $T = 77$ K that we consider in this Letter.

When an open system couples linearly to a harmonic environment, initially in thermal equilibrium at temperature T, the influence of the environment on the reduced system dynamics is fully determined by the BCF $C(t) = \int_0^{\infty} d\omega J(\omega)[\coth(\omega/2k_BT)\cos(\omega t) - i\sin(\omega t)]$ [58]. More specifically, the reduced system density matrix $\rho_s(\tau)$ at a finite time τ is solely determined by $C(t)$ for $0 \leq t \leq \tau$, without any influence from $C(t)$ for $t > \tau$. Therefore, the physical quantities determined by system dynamics over a finite time τ can be simulated by using an effective spectral density instead of an actual one, provided that their BCFs are well matched for $0 \leq t \leq \tau$. This implies that, for accurate simulations of the FMO absorption spectra, one

needs to construct an effective phonon spectral density quantitatively describing the BCF of the full FMO spectral density up to $\tau \approx 300$ fs.

In Fig. 1(b), the Fourier transformed (FT) spectrum of $C(t)$ of the full FMO spectral density at $T = 77$ K over $0 \leq t \leq 300$ fs is shown in blue. Since a sharp cutoff of $C(t)$ at $t = 300$ fs leads to ringing artifacts, we applied a Gaussian filter before the FT, so that the Gaussian-filtered BCF $C(t)e^{-t^2/2\tilde{\sigma}^2}$ with a standard deviation $\tilde{\sigma} = 100$ fs becomes negligible at $t > 3\tilde{\sigma} = 300$ fs. The Gaussian filter also makes the FT spectrum dominated by $C(t)$ at early times, which has more impact on system dynamics than $C(t)$ at later times. Noticeably, the FT spectrum is much less structured than the full FMO spectral density, as the former can be well reproduced by a sum of the Gaussian-filtered BCFs of only six Lorentzian spectral densities, as shown in red in Fig. 1(b), with one representing the contribution of the broad AR spectral density and five describing that of the 62 intrapigment modes [48]. Here the parameters of the effective spectral density, shown in red in Fig. 1(a), were determined in such a way that the total reorganization energy and Huang-Rhys factor of the full FMO spectral density are conserved. Figure 1(c) shows that the BCFs of the effective and full FMO spectral densities are well matched up to $t \approx 300$ fs. We note that a similar degree of reduction in the complexity of phonon spectral densities can be found for other systems (see Supplemental Material [48]).

To demonstrate that the effective spectral density can describe the FMO absorption spectra accurately, we employ DAMPF [9,46] with electronic Hamiltonian H_e of the FMO complex estimated in Ref. [3]. Figure 1(d) shows the absorption spectra of the seven-site FMO model computed by DAMPF based on the full FMO and effective spectral densities, respectively, shown in blue and red, which are quantitatively well matched. Here, the static disorder was treated approximately by computing the optical coherence dynamics using the mean site energies $\langle \epsilon_i \rangle$ of the FMO complex and multiplying it by a Gaussian broadening $e^{-t^2/2\tilde{\sigma}^2}$, so that the coherence decays within $3\tilde{\sigma} = 300$ fs. The use of the effective environmental spectral density described above reduces the computational time (memory cost) from 40 to 3 min (from 400 to 4 MB) when compared to a simulation with the full FMO environment (all simulations were executed using 15 cores in an Intel Xeon 6252 Gold CPU). Since an accurate description of static disorder requires the repetitions of optical coherence simulations with randomly generated site energies, typically requiring $\sim 10^3$ samples, the reduction in computational costs enables one to efficiently and accurately take into account the ensemble dephasing induced by static disorder, as shown as a black dashed line in Fig. 1(d), where the absorption spectra were computed using the effective spectral density and randomly generated site energies ϵ_i. The reduction in computational costs will become even more relevant in molecular parameter estimation, where the mean site energies $\langle \epsilon_i \rangle$ and electronic couplings V_{ij} are optimized until experimental absorption spectra are quantitatively reproduced in simulations [22], thus requiring a much larger number of nonperturbative computations. We note that the computational advantage can become more pronounced for larger vibronic systems with stronger system-environment correlations [48].

So far we have demonstrated how the effective environment can reduce the computational costs of DAMPF and still describe the full environmental effects. Here we discuss how the effective environment approach can impact the computational costs of other existing methods. In conventional HEOM simulations [59], the information about the correlations between system and environments is encoded in a hierarchical structure of auxiliary operators whose dimensions are identical to that of a reduced system density matrix. For a typical PPC model consisting of N pigments, coupled to local vibrational environments modeled by M Lorentzian spectral densities, the total number of auxiliary operators up to the Lth hierarchical layer is given by $(2NM + L)!/(2NM)!/L!$ when the Matsubara terms are not considered [60]. For a dimer ($N = 2$), absorption simulation costs are reduced by almost 5 orders of magnitude, from $\sim$0.27 TB to $\sim$3.8 MB, as the number of Lorentzians is decreased from $M = 62$ to $M = 6$, when a typical hierarchical depth $L = 5$ is considered. For multichromophoric systems consisting of $N = 10$, 20, and 30 pigments, when our effective spectral density with $M = 6$ is considered with $L = 5$, the HEOM simulation costs of absorption simulations are approximately $\sim$0.038, 2.3, and 25 TB, respectively. This may enable HEOM simulations of functionally relevant PPC units, such as the FMO complex ($N = 7$) from green sulfur bacteria [61], the PC645 complex ($N = 8$) from marine algae [45,62], and LH2 ($N = 27$) from purple bacteria [63,64].

To demonstrate that the accuracy of the effective environment approach is insensitive to system parameters, dimer absorption spectra at $T = 77$ K computed by HEOM based on the full FMO and effective spectral densities are shown in Figs. 2(a) and 2(b), respectively, as a function of the electronic coupling $V = V_{12}$. Here the site energies ϵ_i were randomly generated with identical mean values $\langle \epsilon_1 - \epsilon_2 \rangle = 0$, and the transition dipole moments of the two pigments were chosen orthogonal [48]. It is notable that the dimer absorption spectra computed with the effective environment are quantitatively well matched to the full environment model results, over the considered range of the electronic coupling strength V. This shows that accurate absorption spectra can be obtained by using the effective environment constructed based on BCF, independent of the parameters of the system Hamiltonian.

Conventional coarse graining.—Contrary to the BCF-based effective environment, coarse-grained environments

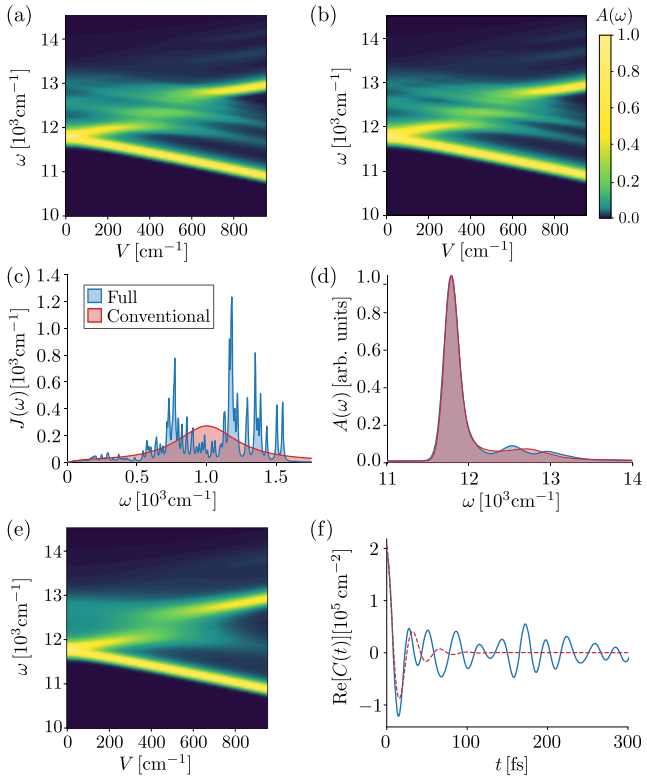

FIG. 2. (a),(b) Dimer absorption spectra at 77 K as a function of electronic coupling V, computed using HEOM with (a) the full FMO and (b) effective spectral densities shown in Fig. 1(a). (c) The full FMO spectral density (blue) and conventional coarse-grained spectral density (red). (d) Monomer absorption spectra at 77 K computed based on the full (blue) and conventional coarse-grained (red) spectral densities. (e) Dimer absorption spectra at 77 K, computed by HEOM with the conventional coarse-grained model. (f) BCFs of the full FMO (blue) and conventional coarse-grained (red) spectral densities at 77 K.

in previous HEOM studies [43–45] have been constructed using different criteria. In Fig. 2(c), a typical coarse-grained environment is shown in red, where the 62 Lorentzian peaks are replaced by a single, broader one. Here the parameters of the broad Lorentzian were determined in such a way that the total reorganization of the 62 intrapigment modes is conserved, and the absorption spectra of monomer ($N = 1$) at 77 K computed with the full and coarse-grained environments are well matched, as shown in Fig. 2(d). It is notable that the dimer absorption spectra computed by HEOM based on the coarse-grained environment, shown in Fig. 2(e), are even qualitatively different from the full environment model results shown in Fig. 2(a). This is due to the significant deviations between the BCFs of the coarse-grained and full FMO spectral density, as shown in Fig. 2(f), thus demonstrating that the conventional criteria for constructing coarse-grained environments are not sufficient to simulate open-system dynamics in a reliable way.

TEDOPA-based coarse graining.—So far we have demonstrated how an effective environment can be constructed for nonperturbative simulation tools where continuous spectral densities are considered. Here we discuss how an effective discrete environment can be systematically constructed for other nonperturbative techniques based on discrete modes.

In thermalized-TEDOPA (T-TEDOPA) [26], a vibrational environment is mapped into a semi-infinite one-dimensional chain of quantum harmonic oscillators, where the electronic states couple only to the first site of the chain and every oscillator interacts only with its nearest neighbors [4,65]. In a crucial step toward the simulation of spectral densities at finite temperature, T-TEDOPA implements a transformed spectral density determined such that all the environmental oscillators in the chain are initialized in their vacuum states and the system dynamics is provably identical to that of the original finite temperature problem [26]. As a consequence, the first oscillator directly coupled to the electronic states is populated at early times and then the population is transferred through the semi-infinite chain. This allows a truncation of the chain in such a way that the BCF is well described within a finite timescale until the population reaches the truncated site, thus ensuring arbitrarily small error in the system observables such as spectra [66]. The finite number of oscillators of the truncated chain results in a discrete phonon spectral density [27]. Figure 3(a) shows the BCF of the truncated T-TEDOPA chain consisting of 51 oscillators, which reproduces the BCF of the full FMO spectral density up to 300 fs (as the number of oscillators increases, the BCF can be reproduced for a longer timescale). The corresponding discrete phonon spectral density, shown in black dots in Fig. 3(b), is qualitatively similar to the effective phonon spectral density constructed based on the previously described FT-based approach with a Gaussian filter. In addition, the discrete spectral density may reduce the computational costs of other nonperturbative tools based on discrete modes. In previous ML-MCTDH simulations of PPCs [33–35], continuous spectral densities in the low-frequency regime were modeled by discrete modes with

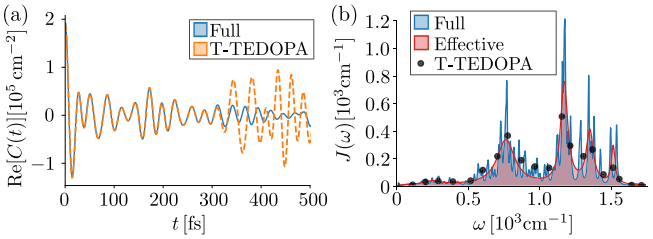

FIG. 3. (a) BCF of the full FMO spectral density at 77 K (blue) and that of a truncated T-TEDOPA chain (orange). (b) Discrete phonon spectral density of the truncated T-TEDOPA chain (black dots) and the full FMO (blue) and effective (red) spectral densities shown in Fig. 1(a).

frequencies equally spaced within an interval of 4 cm^{-1}. When applied to full phonon spectral densities with frequencies up to ~2000 cm^{-1}, this results in several hundreds of discrete modes per site. The number of discrete modes can be dramatically reduced when the T-TEDOPA chain is systematically truncated based on the BCF and timescale of interest, as in the case of absorption simulations requiring only several tens of discrete modes. This is in line with the numerical observations that the chain mapping outperforms other discretization schemes [67].

Conclusions.—We have developed a systematic method to construct effective vibrational environments that describe efficiently electronic dynamics in the presence of highly structured vibrational environments within a finite time interval. When integrated with existing nonperturbative simulation tools, our approach yields a substantial reduction in computational resources, particularly when the environmental correlation time exceeds the timescale of the targeted system dynamics. With increasing simulation timescales, for example, from the subpicosecond timescale of linear optical responses to the picosecond timescale of energy and charge transfer dynamics and nonlinear optical responses, the FT spectrum of the BCF of highly structured vibrational environments grows increasingly complex, revealing the multimodal nature of these environments. Nonetheless, our effective environment construction requires fewer computational resources than modeling the actual environment [48]. The effective environment can be applied in general nonperturbative simulations of multipartite systems coupled to harmonic environments, including polaritonic systems where emitter-photon coupling spectra are highly structured [48,68,69]. This may also support studies concerning the feasibility and resilience of proposed molecular information processors [70] and offer insights into the primary environmental structure responsible for open-system dynamics and its impact on experimentally observable quantities.

We thank Thomas Renger and Ivan Medina for helpful discussions and for providing us with the simulation parameters of the FMO complex and polaritonic systems. This work was supported by the ERC Synergy grant HyperQ (Grant No. 856432), the BMBF project PhoQuant (Grant No. 13N16110), the Quantera project ExtraQt, and the state of Baden-Württemberg through bwHPC and the German Research Foundation (DFG) through Grant No. INST 40/575-1 FUGG (JUSTUS 2 cluster).

*susana.huelga@uni-ulm.de
†martin.plenio@uni-ulm.de

[1] V. May and O. Kühn, *Charge and Energy Transfer Dynamics in Molecular Systems* (Wiley-VCH, New York, 2011).
[2] S. Jang, M. D. Newton, and R. J. Silbey, Multichromophoric Förster resonance energy transfer, Phys. Rev. Lett. **92**, 218301 (2004).
[3] J. Adolphs and T. Renger, How proteins trigger excitation energy transfer in the FMO complex of green sulfur bacteria, Biophys. J. **91**, 2778 (2006).
[4] J. Prior, A. W. Chin, S. F. Huelga, and M. B. Plenio, Efficient simulation of strong system-environment interactions, Phys. Rev. Lett. **105**, 050404 (2010).
[5] J. M. Womick and A. M. Moran, Vibronic enhancement of exciton sizes and energy transport in photosynthetic complexes, J. Phys. Chem. B **115**, 1347 (2011).
[6] E. Romero, V. I. Novoderezhkin, and R. van Grondelle, Quantum design of photosynthesis of bio-inspired solar-energy conversion, Nature (London) **543**, 355 (2017).
[7] S. J. Jang and B. Mennucci, Delocalized excitons in natural light-harvesting complexes, Rev. Mod. Phys. **90**, 035003 (2018).
[8] A. Mattioni, F. Caycedo-Soler, S. F. Huelga, and M. B. Plenio, Design principles for long-range energy transfer at room temperature, Phys. Rev. X **11**, 041003 (2021).
[9] A. D. Somoza, N. Lorenzoni, J. Lim, S. F. Huelga, and M. B. Plenio, Driving force and nonequilibrium vibronic dynamics in charge separation of strongly bound electron-hole pairs, Commun. Phys. **6**, 65 (2023).
[10] L. Zhang, Y. Hao, W. Qin, S. Xie, and F. Qu, Chiral-induced spin selectivity: A polaron transport model, Phys. Rev. B **102**, 214303 (2020).
[11] G.-F. Du, H.-H. Fu, and R. Wu, Vibration-enhanced spin-selective transport of electrons in the DNA double helix, Phys. Rev. B **102**, 035431 (2020).
[12] J. Fransson, Vibrational origin of exchange splitting and chiral-induced spin selectivity, Phys. Rev. B **102**, 235416 (2020).
[13] C. Vittmann, J. Lim, D. Tamascelli, S. F. Huelga, and M. B. Plenio, Spin-dependent momentum conservation of electron-phonon scattering in chirality-induced spin selectivity, J. Phys. Chem. Lett. **14**, 340 (2023).
[14] A. W. Chin, J. Prior, R. Rosenbach, F. Caycedo-Soler, S. F. Huelga, and M. B. Plenio, The role of non-equilibrium vibrational structures in electronic coherence and recoherence in pigment-protein complexes, Nat. Phys. **9**, 113 (2013).
[15] V. Tiwari, W. K. Peters, and D. M. Jonas, Electronic resonance with anticorrelated pigment vibrations drives photosynthetic energy transfer outside the adiabatic framework, Proc. Natl. Acad. Sci. U.S.A. **110**, 1203 (2013).
[16] M. B. Plenio, J. Almeida, and S. F. Huelga, Origin of long-lived oscillations in 2D-spectra of a quantum vibronic model: Electronic versus vibrational coherence, J. Chem. Phys. **139**, 235102 (2013).
[17] A. Chenu, N. Christensson, H. F. Kauffmann, and T. Mančal, Enhancement of vibronic and ground-state vibrational coherences in 2D spectra of photosynthetic complexes, Sci. Rep. **3**, 2029 (2013).
[18] E. Romero, R. Augulis, V. I. Novoderezhkin, M. Ferretti, J. Thieme, D. Zigmantas, and R. van Grondelle, Quantum coherence in photosynthesis for efficient solar-energy conversion, Nat. Phys. **10**, 676 (2014).

[19] F. D. Fuller, J. Pan, A. Gelzinis, V. Butkus, S. S. Senlik, D. E. Wilcox, C. F. Yocum, L. Valkunas, D. Abramavicius, and J. P. Ogilvie, Vibronic coherence in oxygenic photosynthesis, Nat. Chem. **6**, 706 (2014).

[20] V. Butkus, L. Valkunas, and D. Abramavicius, Vibronic phenomena and exciton–vibrational interference in two-dimensional spectra of molecular aggregates, J. Chem. Phys. **140**, 034306 (2014).

[21] J. Lim, D. Paleček, F. Caycedo-Soler, C. N. Lincoln, J. Prior, H. von Berlepsch, S. F. Huelga, M. B. Plenio, D. Zigmantas, and J. Hauer, Vibronic origin of long-lived coherence in an artificial molecular light harvester, Nat. Commun. **6**, 7755 (2015).

[22] F. Caycedo-Soler, A. Mattioni, J. Lim, T. Renger, S. F. Huelga, and M. B. Plenio, Exact simulation of pigment-protein complexes unveils vibronic renormalization of electronic parameters in ultrafast spectroscopy, Nat. Commun. **13**, 2912 (2022).

[23] F. C. Spano, The spectral signatures of Frenkel polarons in H- and J-aggregates, Acc. Chem. Res. **43**, 429 (2010).

[24] L. Farouil, F. Alary, E. Bedel-Pereira, and J.-L. Heully, Revisiting the vibrational and optical properties of P3HT: A combined experimental and theoretical study, J. Phys. Chem. A **122**, 6532 (2018).

[25] M. S. Barclay, J. S. Huff, R. D. Pensack, P. H. Davis, W. B. Knowlton, B. Yurke, J. C. Dean, P. C. Arpin, and D. B. Turner, Characterizing mode anharmonicity and Huang-Rhys factors using models of femtosecond coherence spectra, J. Phys. Chem. Lett. **13**, 5413 (2022).

[26] D. Tamascelli, A. Smirne, J. Lim, S. F. Huelga, and M. B. Plenio, Efficient simulation of finite-temperature open quantum systems, Phys. Rev. Lett. **123**, 090402 (2019).

[27] A. Nüßeler, D. Tamascelli, A. Smirne, J. Lim, S. F. Huelga, and M. B. Plenio, Fingerprint and universal Markovian closure of structured bosonic environments, Phys. Rev. Lett. **129**, 140604 (2022).

[28] I. de Vega and M. Bañuls, Thermofield-based chain-mapping approach for open quantum systems, Phys. Rev. A **92**, 052116 (2015).

[29] T. Chen, V. Balachandran, C. Guo, and D. Poletti, Steady-state quantum transport through an anharmonic oscillator strongly coupled to two heat reservoirs, Phys. Rev. E **102**, 012155 (2020).

[30] H.-D. Meyer, U. Manthe, and L. Cederbaum, The multi-configurational time-dependent Hartree approach, Chem. Phys. Lett. **165**, 73 (1990).

[31] H. Wang and M. Thoss, Multilayer formulation of the multiconfiguration time-dependent Hartree theory, J. Chem. Phys. **119**, 1289 (2003).

[32] H. Wang and M. Thoss, From coherent motion to localization: Dynamics of the spin-boson model at zero temperature, New J. Phys. **10**, 115005 (2008).

[33] J. Schulze and O. Kühn, Explicit correlated exciton-vibrational dynamics of the FMO complex, J. Phys. Chem. B **119**, 6211 (2015).

[34] J. Schulze, M. F. Shibl, M. J. Al-Marri, and O. Kühn, Multi-layer multi-configuration time-dependent Hartree (ML-MCTDH) approach to the correlated exciton-vibrational dynamics in the FMO complex, J. Chem. Phys. **144**, 185101 (2016).

[35] J. Schulze, M. F. Shibl, M. J. Al-Marri, and O. Kühn, The effect of site-specific spectral densities on the high-dimensional exciton-vibrational dynamics in the FMO complex, Chem. Phys. **497**, 10 (2017).

[36] M. F. Shibl, J. Schulze, M. J. Al-Marri, and O. Kühn, Multilayer-MCTDH approach to the energy transfer dynamics in the LH2 antenna complex, J. Phys. B **50**, 184001 (2017).

[37] M. Schröter, S. D. Ivanov, J. Schulze, S. P. Polyutov, Y. Yan, T. Pullerits, and O. Kühn, Exciton–vibrational coupling in the dynamics and spectroscopy of Frenkel excitons in molecular aggregates, Phys. Rep. **567**, 1 (2015).

[38] A. Strathearn, P. Kirton, D. Kilda, J. Keeling, and B. W. Lovett, Efficient non-Markovian quantum dynamics using time-evolving matrix product operators, Nat. Commun. **9**, 3322 (2018).

[39] R. Rosenbach, J. Cerrillo, S. F. Huelga, J. Cao, and M. B. Plenio, Efficient simulation of non-Markovian system-environment interaction, New J. Phys. **18**, 023035 (2016).

[40] Y. Tanimura and R. Kubo, Time evolution of a quantum system in contact with a nearly Gaussian–Markoffian noise bath, J. Phys. Soc. Jpn. **58**, 101 (1989).

[41] A. Ishizaki and G. R. Fleming, Theoretical examination of quantum coherence in a photosynthetic system at physiological temperature, Proc. Natl. Acad. Sci. U.S.A. **106**, 17255 (2009).

[42] J. Strümpfer and K. Schulten, Light harvesting complex II B850 excitation dynamics, J. Chem. Phys. **131**, 225101 (2009).

[43] C. Kreisbeck and T. Kramer, Long-lived electronic coherence in dissipative exciton dynamics of light-harvesting complexes, J. Phys. Chem. Lett. **3**, 2828 (2012).

[44] C. Kreisbeck, T. Kramer, and A. Aspuru-Guzik, Scalable high-performance algorithm for the simulation of exciton dynamics. Application to the light-harvesting complex ii in the presence of resonant vibrational modes, J. Chem. Theory Comput. **10**, 4045 (2014).

[45] S. M. Blau, D. I. G. Bennett, C. Kreisbeck, G. D. Scholes, and A. Aspuru-Guzik, Local protein solvation drives direct down-conversion in phycobiliprotein PC645 via incoherent vibronic transport, Proc. Natl. Acad. Sci. U.S.A. **115**, E3342 (2018).

[46] A. D. Somoza, O. Marty, J. Lim, S. F. Huelga, and M. B. Plenio, Dissipation-assisted matrix product factorization, Phys. Rev. Lett. **123**, 100502 (2019).

[47] M. Rätsep and A. Freiberg, Electron phonon and vibronic couplings in the FMO bacteriochlorophyll a antenna complex studied by difference fluorescence line narrowing, J. Lumin. **127**, 251 (2007).

[48] See Supplemental Material at http://link.aps.org/supplemental/10.1103/PhysRevLett.132.100403 for more detailed information on the phonon spectral densities of the FMO complex considered in simulations, the theory of absorption spectra, the simulation-time dependence of coarse graining, the timescale analysis of absorption spectra of the FMO complex, the coarse graining of emitter-photon interaction, and the computational costs of DAMPF: the FMO complex and linear chains, which includes Refs. [49–57].

[49] D. Tamascelli, A. Smirne, S. F. Huelga, and M. B. Plenio, Nonperturbative treatment of non-Markovian dynamics of

open quantum systems, Phys. Rev. Lett. **120**, 030402 (2018).
[50] F. Mascherpa, A. Smirne, A. D. Somoza, P. Fernández-Acebal, S. Donadi, D. Tamascelli, S. F. Huelga, and M. B. Plenio, Optimized auxiliary oscillators for the simulation of general open quantum systems, Phys. Rev. A **101**, 052108 (2020).
[51] S. Mukamel, *Principles of Nonlinear Optical Spectroscopy* (Oxford University Press, New York, 1995).
[52] D. M. Jonas, Two-dimensional femtosecond spectroscopy, Annu. Rev. Phys. Chem. **54**, 425 (2003).
[53] T. Brixner, T. Mančal, I. V. Stiopkin, and G. R. Fleming, Phase-stabilized two-dimensional electronic spectroscopy, J. Chem. Phys. **121**, 4221 (2004).
[54] G. Panitchayangkoon, D. Hayes, K. A. Fransted, J. R. Caram, E. Harel, J. Wen, R. E. Blankenship, and G. S. Engel, Long-lived quantum coherence in photosynthetic complexes at physiological temperature, Proc. Natl. Acad. Sci. U.S.A. **107**, 12766 (2010).
[55] V. Zazubovich, I. Tibe, and G. J. Small, Bacteriochlorophyll a Franck-Condon factors for the S0-S1(Qy) transition, J. Phys. Chem. B **105**, 12410 (2001).
[56] J. Pieper, M. Rätsep, I. Trostmann, H. Paulsen, G. Renger, and A. Freiberg, Excitonic energy level structure and pigment-protein interactions in the recombinant water-soluble chlorophyll protein. I. Difference fluorescence line-narrowing, J. Phys. Chem. B **115**, 4042 (2011).
[57] B. Stuart, *Infrared Spectroscopy: Fundamentals and Applications* (Wiley, New York, 2005).
[58] R. P. Feynman and F. L. Vernon, The theory of a general quantum system interacting with a linear dissipative system, Ann. Phys. (N.Y.) **24**, 118 (1963).
[59] T. Kramer, M. Noack, A. Reinefeld, M. Rodríguez, and Y. Zelinskyy, Efficient calculation of open quantum system dynamics and time-resolved spectroscopy with distributed memory HEOM (DM-HEOM), J. Comput. Chem. **39**, 1779 (2018).
[60] J. Lim, C. M. Bösen, A. D. Somoza, C. P. Koch, M. B. Plenio, and S. F. Huelga, Multicolor quantum control for suppressing ground state coherences in two-dimensional electronic spectroscopy, Phys. Rev. Lett. **123**, 233201 (2019).
[61] M. T. W. Milder, B. Brüggemann, R. van Grondelle, and J. L. Herek, Revisiting the optical properties of the FMO protein, Photosynth. Res. **104**, 257 (2010).
[62] E. Collini, C. Y. Wong, K. E. Wilk, P. M. G. Curmi, P. Brumer, G. D., and Scholes, Coherently wired light-harvesting in photosynthetic marine algae at ambient temperature, Nature (London) **463**, 644 (2010).
[63] G. D. Scholes, I. R. Gould, R. J. Cogdell, and G. R. Fleming, Ab initio molecular orbital calculations of electronic couplings in the LH2 bacterial light-harvesting complex of *Rps. acidophila*, J. Phys. Chem. B **103**, 2543 (1999).
[64] C. J. Law, A. W. Roszak, J. Southall, A. T. Gardiner, N. W. Isaacs, and R. J. Cogdell, The structure and function of bacterial light-harvesting complexes (review), Mol. Membr. Biol. **21**, 183 (2004).
[65] A. W. Chin, A. Rivas, S. F. Huelga, and M. B. Plenio, Exact mapping between system-reservoir quantum models and semi-infinite discrete chains using orthogonal polynomials, J. Math. Phys. (N.Y.) **51**, 092109 (2010).
[66] F. Mascherpa, A. Smirne, S. F. Huelga, and M. B. Plenio, Open systems with error bounds: Spin boson model with spectral density variations, Phys. Rev. Lett. **118**, 100401 (2017).
[67] I. de Vega, U. Schollwöck, and F. A. Wolf, How to discretize a quantum bath for real-time evolution, Phys. Rev. B **92**, 155126 (2015).
[68] J. del Pino, F. A. Y. N. Schröder, A. W. Chin, J. Feist, and F. J. Garcia-Vidal, Tensor network simulation of non-Markovian dynamics in organic polaritons, Phys. Rev. Lett. **121**, 227401 (2018).
[69] I. Medina, F. J. García-Vidal, A. I. Fernández-Domínguez, and J. Feist, Few-mode field quantization of arbitrary electromagnetic spectral densities, Phys. Rev. Lett. **126**, 093601 (2021).
[70] M. R. Wasielewski, M. D. E. Forbes, N. L. Frank, K. Kowalski, G. D. Scholes, J. Yuen-Zhou, M. A. Baldo, D. E. Freedman, R. H. Goldsmith, T. Goodson III, M. L. Kirk, J. K. McCusker, J. P. Ogilvie, D. A. Shultz, S. Stoll, and K. B. Whaley, Exploiting chemistry and molecular systems for quantum information science, Nat. Rev. Chem. **4**, 490 (2020).